

LA-UR-19-29354 (Accepted Manuscript)

An Analysis of Limiting Cases for the Metal Oxide Film Growth Kinetics Using an Oxygen Defects Model Accounting for Transport and Interfacial Reactions

Samin, Adib Jamil Taylor, Christopher D.

Provided by the author(s) and the Los Alamos National Laboratory (2019-09-17).

To be published in: Journal of Non-Equilibrium Thermodynamics

DOI to publisher's version: 10.1515/jnet-2018-0018

Permalink to record: http://permalink.lanl.gov/object/view?what=info:lanl-repo/lareport/LA-UR-19-29354

Disclaimer:

Los Alamos National Laboratory, an affirmative action/equal opportunity employer, is operated by Triad National Security, LLC for the National Nuclear Security Administration of U.S. Department of Energy under contract 89233218CNA000001. By approving this article, the publisher recognizes that the U.S. Government retains nonexclusive, royalty-free license to publish or reproduce the published form of this contribution, or to allow others to do so, for U.S. Government purposes. Los Alamos National Laboratory requests that the publisher identify this article as work performed under the auspices of the U.S. Department of Energy. Los Alamos National Laboratory strongly supports academic freedom and a researcher's right to publish; as an institution, however, the Laboratory does not endorse the viewpoint of a publication or guarantee its technical correctness.

An analysis of limiting cases for the metal oxide film growth kinetics using an oxygen defects model accounting for transport and interfacial reactions

Adib J. Samin^a and Christopher D. Taylor^b

^a Materials Science and Technology Division, Los Alamos National Laboratory,

Los Alamos, New Mexico 87545, USA

^b Department of Materials Science and Engineering, The Ohio State University

2041 College Rd Columbus, OH 43210

Abstract:

This work was motivated by the need to understand the passivation of metal surfaces to provide resistance against chemical degradation, given that corrosion is a major limiting factor in the operational lifetime of metals and their alloys. In this study, a unified analysis for an oxide growth model was presented. The oxide growth model was consistent with the literature and accounted for the transport of oxygen defects through a growing oxide film, as well as the electrochemical reactions of oxygen defects at the metal/oxide and oxide/environment interfaces. A linear potential profile across the oxide film was assumed. The model was analyzed for different rate-limiting steps in the physicochemical process and perturbation techniques were utilized when necessary. The investigation yielded the well-known linear, parabolic, logarithmic and integral rate laws and the conditions that led to these rate laws were discussed.

Introduction:

Corrosion is an important performance-limiting factor for metals and their alloys, particularly under extreme conditions such as nuclear reactor environments, turbine systems, long term storage of hazardous materials or oil and gas handling. The so-called "passivation" of a metal or alloy surface with respect to corrosion occurs when a stable protective oxide film forms on its surface

hindering further corrosion of the metal. Therefore, predictive modeling of the kinetics of oxide growth has emerged as a matter of great significance to various engineering and industrial applications. Establishing accurate analytical or numerical models for passivity would be a core component for next-generation integrated computational material engineering (ICME) approaches to corrosion resistant alloy (CRA) design and optimization.

Over the past century, a large number of investigators have sought to uncover the different mechanisms involved in metal oxide growth. Wagner in 1933 [1] was one of the pioneers in attempting to develop a theoretical understanding of oxidation kinetics. Subsequently the Mott-Cabrera model [2] was proposed and in that model the authors assumed the transport of metal cations through oxide film was the rate-limiting step and that the activation energy of this step was reduced by the electric field in the oxide film. This model led to a parabolic time dependence in the limit of a weak field (thick oxides). In the limit of thin oxides (thin oxides), the limiting step was assumed to be the injection of cations into the oxide film and this led to an inverse logarithmic growth law.

Fehlner and Mott [3] subsequently modified the model by assuming that anion transport was the rate limiting step and the activation energy for the process was assumed to increase linearly with the oxide thickness. Furthermore, the model assumed the strength of the electric field to be constant in the oxide and independent of thickness. This model predicted a logarithmic rate law. Sato and Cohen [4] proposed a place exchange mechanism to explain their experimental data and this approach also yielded a logarithmic rate law.

Macdonald et al. [5] developed and then continually improved [6] the point defect model (PDM) to study oxide film kinetics. The model assumed a linear potential profile in the oxide film in addition to accounting for potential drops across the interfaces. The original version of the model

assumed that the transport of anionic vacancies across the oxide was responsible for the oxide growth. This led to a logarithmic rate law. In an extension of the model [7], Macdonald considered the case where the growth was controlled by interfacial reactions and this yielded another logarithmic rate law. Sun et al. [8] incorporated dissolution to the PDM to account for steady state oxide film thickness.

Marcus et al.[9, 10] developed a Generalized Growth Model (GGM) in which the transport of anions and cations was considered and the time dependent behavior of film was explored in contrast to the quasi-steady approximation. The authors recovered parabolic rate laws for both thin and thick oxides whereas the rate laws for intermediate oxides were determined via numerical integration. The authors were also successful in recovering linear time dependence for the case where the growth was limited by the injection of cations at the metal/oxide interface.

Suo et al. [11] conducted a mathematical analysis on the kinetics of oxidation growth. In that work, the authors did not use the quasi-steady state approximation but rather treated the variation of the boundary using the Landau transformation. In this work, the authors used perturbation methods to analyze the problem and recovered a parabolic dependence on time in the limit of fast interfacial kinetics. However, the authors in this work did not take into account the role of migration in the transport and did not account for the electrochemical nature of the interfacial reactions.

Baroody et al. [12] recently presented a well-developed model for oxide formation and growth on platinum. The model was based on the transport of oxygen vacancies and a parametric analysis of the model was performed. The authors were successful in reproducing a wide range of growth laws observed in the experimental literature. However, the authors in this work accounted for the electrochemical nature of the interactions at the interfaces by utilizing an ad hoc hyperbolic tangent

function at the metal/oxide interface in an attempt to produce reasonable results. Furthermore, the approach followed by the authors employed the quasi-static approximation.

From the overview of the available literature, it is clear that different kinetic laws have been observed in different models for different limiting cases. In this work, we will present a mathematical analysis of the limiting steps in oxide film growth kinetics in an attempt to reconcile the different rate laws observed. We will start by building on Baroody's recent model by first modifying it to account for the electrochemical nature of the interactions at the interfaces and also by considering the fully unsteady situation when possible. The goal is to analyze extreme cases and rigorously derive time dependences for the oxide film growth in different regimes. In this work we will ignore the role of pH and variations in the applied potential to keep the problem tractable and amenable to analytical solutions.

Mathematical Analysis, Results and Discussion:

Model Description:

In the present model which is inspired by the ideas of the point defect model and particularly by some of the ideas of the oxide growth model recently presented by Baroody et al. [12], only one species is tracked namely oxygen defects. These unfilled oxygen defects are produced at the metal/oxide interface via an oxidation reaction of the form:

$$V \xrightarrow{k_1} V^{n+} + ne^- \qquad (I)$$

These defects then transport through the length of the oxide and are finally annihilated at the oxide solution interface through a reduction reaction of the form:

$$V^{n+} + ne^{-} \xrightarrow{k_2} V \qquad (II)$$

In the model, the oxide can only grow at the metal/solution interface hence the x=0 boundary at the metal/oxide interface is fixed, and the oxide can only grow at the x=L(t) end located at the oxide/solution where the defects may recombine with adsorbed oxygen atoms on the oxide surface. An illustration is included in figure 1. In this study, C_V denotes the concentration of the filled oxygen defects and C denotes the concentration of the oxygen vacancies V^{n+} . In a future work, the motion of metal defects in the opposite direction will be accounted for. However, this was neglected for now to enable analytical manipulations.

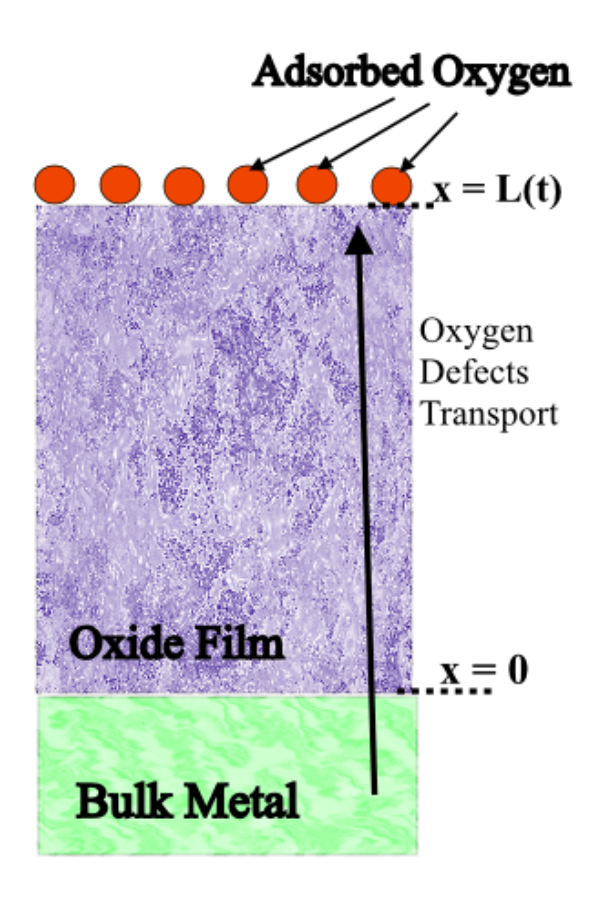


Figure 1. An illustration of the model used in the study

The present model assumes that the potential is a linear function with respect to the oxide position consistent with the PDM model. This assumption was indeed shown to be a good

assumption when the Poisson equation was solved along with the Nernst-Planck equations for the different species [13]. Accordingly, the potential function in the oxide film will be assumed to be of the form:

$$\phi(x) = \phi_1 - mx$$

In the equation for the potential $\phi_1 > 0$ is the potential at the metal/oxide end of the oxide film (at x = 0) and m > 0 is a positive number so that the potential drops towards the oxide/solution interface. The metal itself is considered to be held at a potential of E and the potential at the solution is zero.

Another important process which plays a role in determining the oxide thickness is the thinning of the oxide due to the interaction of the oxide with the solution. This process has been postulated to be a function of the pH of the solution and helps establish a steady state thickness for the oxide. This process however is not expected to play an important role in the initial stages of oxide growth and will not be considered for now.

In this simple model there are three different processes involved in the kinetics of the oxide growth process, namely the production of the oxygen defects at the metal/oxide interface, the transport of the defects through the oxide, and the kinetics involved in the recombination reaction at the oxide/solution interface.

Limiting Cases:

The goal of this work is to present the functional form for the dependence of the oxide thickness growth on time for several limiting cases and thus giving a theoretical explanation for the different experimentally-observed time dependences of the oxide growth reported in the literature. It is well-known that the kinetics of a multi-step process is determined by the rate-limiting step (the slowest

step) and as such we will consider different cases in this work where each of the aforementioned processes may be the rate-determining step in the oxide film growth.

Case 1: The oxygen defect production (at x = 0) is the rate limiting step:

Reaction (1) at the metal/oxide interface is an oxidation reaction which is associated with the transfer of charge and in this case we may use the Butler-Volmer equation to describe the kinetics of the process. Accordingly, we have the boundary condition:

$$\frac{dL}{dt} = AC_V k_1^0 \exp\left(\frac{(1-\alpha)nF}{R_u T}(E - \phi(0))\right) - Q \quad ; \quad L(0) = 0$$
 (1)

As we alluded to earlier, Q is a term accounting for the thinning of the oxide and is assumed to be a function of the solution pH and the thickness of the oxide film and we hypothesize that it assumes the following form:

$$Q = \begin{cases} 0 & if \ L(t) \le L_{crit} \\ f(pH) & otherwise \end{cases}$$
 (2)

As mentioned before, we will focus our attention in this study on the early stages of oxide growth and as such we set Q=0 in equation 1. In equation (1), A is the cross sectional area, C_V is the concentration of metal atoms that will give rise to the oxygen vacancies and which is assumed to be held constant at the bulk value $C_V=C_\infty$ (where C_∞ is the concentration of the bulk metal) and from our definition of the potential in the previous section we find that $\phi(0)=\phi_1$ (a constant). The other terms in reaction 1 involve k_1^0 which is the reaction rate constant at the formal potential (with units of cm²/s), α is the charge transfer coefficient, T is the temperature and R_u is the universal gas constant. The initial conditions for the oxide thickness are also given. Therefore, we may write the solution as:

$$L(t) = AC_{\infty}k_1^0 \exp\left(\frac{(1-\alpha)nF}{R_nT}(E-\phi_1)\right) * t$$
(3)

By examining equation (3) we observe that we recover the linear dependence on time $L(t) \propto t$. This analysis agrees with the conclusion of the analysis by Marcus et al. [9].

Case 2: The oxygen defect annihilation (at x = L(t)) is the rate limiting step:

In this case we write the equation for the oxide thickness according to Butler-Volmer kinetics, where the kinetics of the reduction reaction occurring at the oxide solution boundary become given by the equation:

$$\frac{dL}{dt} = AC(x = L(t), t)k_2^0 \exp\left(\frac{-\alpha nF}{R_u T} \left(0 - \phi(L(t))\right)\right) - Q \quad ; \quad L(0) = 0$$
(4)

In equation 4, C actually represents the concentration of the charged oxygen defect (Vⁿ⁺) which we track in this model and which transports across the oxide film. In this particular case study, we now assume that the transport process is much faster than the kinetics of the reaction at the oxide/solution interface and therefore we write $C(x = L(t), t) = C_{\infty}$. Throughout this study we are only interested in the early stages of oxide growth so, again, we set Q = 0. Finally, the potential at the oxide/solution end of the oxide is: $\phi(L(t)) = \phi_1 - mL(t)$ (from our assumption regarding the linear form of the potential). Hence we may write:

$$\frac{dL}{dt} = AC_{\infty}k_2^0 \exp\left(\frac{-\alpha nF}{R_u T}(-\phi_1 + mL(t))\right) \quad ; \quad L(0) = 0$$
 (5)

By solving the separable initial value problem indicated by (5) we arrive at:

$$L(t) = \frac{1}{mP} ln(Rt+1) \tag{6}$$

where we used the symbol $R = mPAC_{\infty}k_2^0exp\left(\frac{\alpha nF\phi_1}{R_uT}\right)$ and the dimensionless quantity $P = \frac{\alpha nF}{R_uT}$. From this analysis we arrive at a logarithmic rate law.

Case 3: The transport of oxygen defects through the oxide is the rate limiting step:

In our discussion, we will use our assumption of a known linear potential function $(x) = \phi_1 - mx$. Hence, we may write the governing Nernst-Planck equation for the transport of oxygen defects (concentration C) through the oxide as:

$$\frac{\partial C}{\partial t} = D \frac{\partial^2 C}{\partial x^2} - mD \frac{zF}{R_u T} \frac{\partial C}{\partial x}$$
 (7)

In this limiting case, the reaction rates at both interfaces are assumed to be extremely fast in comparison with the transport. Hence, the defect concentration at the metal/oxide interface is always available at bulk concentration and any defects that reach the oxide/solution interface are quickly annihilated and thus an appropriate choice for the boundary conditions is:

$$C(0,t) = C_{\infty}$$
 and $C(L,t) = 0$ (8)

Finally, the change of the oxide film thickness in the model is assumed to be proportional to the flux at the oxide/environment interface hence:

$$\frac{dL}{dt} = \beta_1 \left(-D \frac{\partial C}{\partial x} \Big|_{x=L(t)} \right) \quad ; \quad L(0) = 0$$
 (9)

In equation (9), the migration term's contribution to the flux at x=L(t) vanishes given the boundary conditions in equation (8) (since C(L, t) = 0)

We start our analysis by non-dimensionalizing the problem described by equations 7,8, and 9. We use the following quantities:

$$X = \frac{x}{L_0} ; Y = \frac{L}{L_0} ; \tau = \frac{tD}{L_0^2} ; U = \frac{\phi}{U_0} ;$$

$$\rho = \frac{c}{c_\infty} ; M = m \frac{L_0}{U_0} ; P = \frac{zF}{R_0 T} ; \beta = C_\infty \beta_1$$
(10)

By transforming the equations, the dimensionless problem assumes the form:

$$\frac{\partial \rho}{\partial \tau} = \frac{\partial^2 \rho}{\partial X^2} - M U_0 P \frac{\partial \rho}{\partial X} \tag{11}$$

$$\rho(0,\tau) = 1$$
 ; $\rho(Y,\tau) = 0$; $\frac{dY}{d\tau} = -\beta \frac{\partial \rho}{\partial X}\Big|_{X=Y(\tau)}$; $Y(0) = 0$ (12)

Typically, P is expected to be of order of magnitude O(10) or O(1) (C/J) for room temperature and elevated temperatures respectively. The reference potential U_0 usually ranges between O(1) and O(10⁻²) Volts [10] and M is of order O(1). Finally, the oxide thickness growth is typically on the order of tens of nm per year [14], but can be much faster on the order of O(10⁻¹³) cm/s [10] and the diffusivity of the oxygen defects in the oxide is of order O(10⁻²⁰) cm²/s [10, 13] but this number depends on the temperature and increases for higher temperatures. The typical concentration of the oxygen vacancies in the oxide is on the order of about (10⁻² mol/cm³) [10, 12] hence, β may span several orders of magnitude from O(10⁻⁴) to O(10²). Therefore, we can consider a few distinct limiting cases:

Case 3a: $MU_0P \ll \beta \ll 1$

If: $MU_0P\sim O(\epsilon^2)$ and $\beta\sim O(\epsilon)$ where $\epsilon=10^{-1}$ and if we re-express $\rho(X,\tau)$ as a function of $\rho(X,Y)$ instead we can write:

$$\frac{\partial \rho}{\partial Y} \frac{dY}{d\tau} = \frac{\partial^2 \rho}{\partial X^2} - \epsilon^2 \frac{\partial \rho}{\partial X}$$

$$\rho(0,\tau) = 1 \quad ; \quad \rho(Y,\tau) = 0 \quad ; \quad \frac{dY}{d\tau} = -\epsilon \frac{\partial \rho}{\partial X}\Big|_{X=Y(\tau)} \quad ; \quad Y(0) = 0$$
(13)

This problem corresponds to the case where diffusion dominates the transport process and the effect of migration is small. The problem is reformulated as:

$$\left(-\epsilon \frac{\partial \rho}{\partial X}\Big|_{X=Y(\tau)}\right) \frac{\partial \rho}{\partial Y} = \frac{\partial^2 \rho}{\partial X^2} - \epsilon^2 \frac{\partial \rho}{\partial X}$$

$$\rho(0,\tau) = 1 \quad ; \quad \rho(Y,Y) = 0 \quad ; \qquad \frac{dY}{d\tau} = -\epsilon \frac{\partial \rho}{\partial X}\Big|_{X=Y(\tau)} \quad ; \quad Y(0) = 0$$

$$(14)$$

We seek a regular perturbation solution of the form:

$$\rho(X,Y) = \rho_0(X,Y) + \epsilon \rho_1(X,Y) + \epsilon^2 \rho_2(X,Y) + \cdots$$

Hence we can write an approximate perturbed solution to problem 13 (see appendix A for details) as:

$$\rho(X,Y) = 1 - \frac{X}{Y} + \epsilon \left(\frac{X^3}{6Y^3} - \frac{X}{6Y}\right) + O(\epsilon^2)$$
(15)

Furthermore, the oxide thickness is given by (Appendix A):

$$Y(\tau) = \sqrt{2\epsilon\tau - \frac{2}{3}\epsilon^2\tau}$$
 (16)

Thus, we recover the experimentally observed time dependence of the form $L(t) \propto \sqrt{t}$ consistent with the Mott-Cabrera model.

Case 3b: $\beta \ll MU_0P \approx O(1)$

This is the case where migration and diffusion are both important for the transport process and the oxide thickness changes slowly. In this case, we denote $MU_0P = G$ which is of order O(1), and the problem is cast in the form:

$$\frac{\partial \rho}{\partial Y} \left(-\epsilon \frac{\partial \rho}{\partial X} \Big|_{X = Y(\tau)} \right) = \frac{\partial^2 \rho}{\partial X^2} - G \frac{\partial \rho}{\partial X}$$

$$\rho(0, \tau) = 1 \quad ; \quad \rho(Y, \tau) = 0 \quad ; \qquad \frac{dY}{d\tau} = -\epsilon \frac{\partial \rho}{\partial X} \Big|_{X = Y(\tau)} \quad ; \quad Y(0) = 0$$
(17)

And to leading order we obtain (see Appendix B):

$$Y + \frac{1}{G}e^{-GY} - \frac{1}{G} = \epsilon G\tau \tag{18}$$

This is similar to the integral rate law which emerges from the PDM model [15]. For oxide layers that are thick enough, this equation reduces to the linear growth law. The equation was solved numerically for different values of G and ϵ . The results are included in figure 2 below and are consistent with the literature [12].

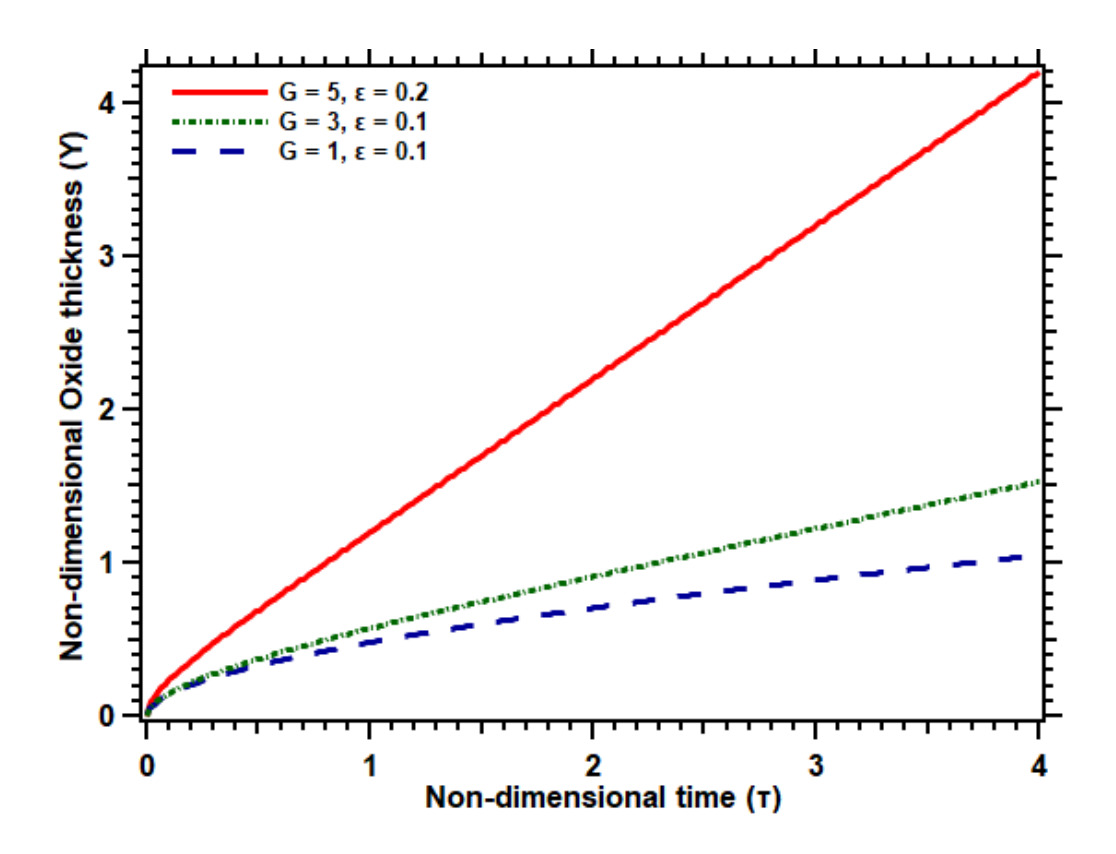


Figure 2. The oxide growth for case 3b described by equation 28 plotted for different values of G and ϵ .

<u>Case 3C:</u> $G \gg 1 \gg \beta$ (The case where migration dominates over diffusion)

This version of the problem yields the following boundary value problem:

$$\frac{\partial \rho}{\partial Y} \left(-\epsilon^2 \frac{\partial \rho}{\partial X} \Big|_{X = Y(\tau)} \right) = \epsilon \frac{\partial^2 \rho}{\partial X^2} - \frac{\partial \rho}{\partial X}$$
(19)

$$\rho(0,\tau) = 1 \quad ; \quad \rho(Y,\tau) = 0 \quad ; \qquad \frac{dY}{d\tau} = -\epsilon^2 \frac{\partial \rho}{\partial X} \bigg|_{X = Y(\tau)} \quad ; \quad Y(0) = 0$$

This is a singular perturbation problem and its solution (Appendix C), yields a linear dependence $Y \propto \tau$ in the form:

$$Y = (\epsilon + \epsilon^3)\tau + O(\epsilon^4)$$
 (20)

Discussion

The above mathematical analysis shows that, starting with a single model and solving under various limiting conditions, a variety of phenomena can be predicted for oxide growth rate laws.

To summarize:

In case 1 the oxygen defect production at the oxide/metal interface led to a linear dependence on time. Case 2 explored the situation where oxygen defect annihilation at the oxide/environment interface was the rate-limiting step and this gave rise to a logarithmic rate law. In case 3 we considered the transport of oxygen defects through the oxide to be the rate limiting step and in this case we studied three distinct sub-cases. In the first subcase 3a, diffusion was dominant over migration and this gave rise to a parabolic dependence. In case 3b, diffusion and migration were both equally important and this case led to an integral rate law. Finally, subcase 3c considered the situation were migration dominated the transport process and this yielded a singular perturbation problem which eventually led to a linear rate law. For all these cases considering transport as the limiting process for oxide growth, the oxide growth was assumed to be slowly varying with the flux of oxygen defects at the oxide/environment interface.

These results are consistent with experimental observations in the literature. For example, Chandrasekharan et al. [16] studied the thermal oxidation of tantalum films of various oxidation states from 300 to 700 °C. The authors observed the growth rate of the oxide to be logarithmic at 300 °C, parabolic at 500 °C and then a multistep growth behavior (a combination of parabolic and linear growth at 700 °C. Unutulmazsoy et al. [17] examined the oxidation kinetics of thin nickel films between 250 and 500 °C. The authors observed a parabolic growth rate which

indicated that the process was diffusion-controlled and further noticed accelerated Ni diffusion along the grain boundaries. Dighton and Miley[18] showed that copper may oxidize parabolically over a limited thickness range and then change to a logarithmic growth rate.

Next generation versions of the model would incrementally add complexity, and hence, further realism to the model. Consequently, however, the convenience of obtaining an analytical solution to the model would be replaced with the need for numerical solutions. Examples of the development that could be pursued, in approximate order of increasing complexity, include:

- a) Direct solution of the potential across the oxide instead of assumption of a linear drop.
- b) Include the possibility for cation transport.
- c) Develop the model for alloys by allowing for multiple types of cations transporting
- d) Consider phase transitions within the oxide film, such that inner and outer films of different composition, stoichiometry and transport properties could be considered
- e) Consider the formation of phases other than oxides (i.e. sulfides or carbonates for metals in oil and gas conditions)
- f) Develop models that incorporate the physics of microstructure (such as grain boundaries)
- g) Include the role of mechanical stresses that build up during oxide growth
- h) Simulation of porosity and microcracks in oxides that will influence the transport of ions and solution across porous or cracked oxide films

Obviously some of these factors will be significantly more complex and require the use of 2D and 3D models to describe increasingly realistic scenarios.

Appendix A:

By plugging this proposed solution into the governing equation of problem 14 we find that:

The O(1) problem:

$$0 = \frac{\partial^2 \rho_0}{\partial X^2} \tag{A1}$$

$$\rho_0(0,Y) = 1 \ \ \, ; \ \ \, \rho_0\left(Y,Y\right) = 0$$

The $O(\epsilon)$ problem:

$$\left(-\frac{\partial \rho_0}{\partial X} \Big|_{X = Y(\tau)} \right) \frac{\partial \rho_0}{\partial Y} = \frac{\partial^2 \rho_1}{\partial X^2}$$

$$\rho_1(0, \tau) = 0 \quad ; \quad \rho_1(Y, Y) = 0$$
(A2)

The $O(\epsilon^2)$ problem:

$$\left(-\frac{\partial \rho_1}{\partial X}\Big|_{X=Y(\tau)}\right) \frac{\partial \rho_0}{\partial Y} + \left(-\frac{\partial \rho_0}{\partial X}\Big|_{X=Y(\tau)}\right) \frac{\partial \rho_1}{\partial Y} = \frac{\partial^2 \rho_2}{\partial X^2} - \frac{\partial \rho_0}{\partial X}$$

$$\rho_2(0,\tau) = 0 \quad ; \quad \rho_2(Y,Y) = 0$$
(A3)

And so on...

The solution satisfying problem A1 may be expressed as:

$$\rho_0(X,Y) = 1 - \frac{X}{Y} \tag{A4}$$

The solution to problem A2 is:

$$\rho_1(X,Y) = \frac{X^3}{6Y^3} - \frac{X}{6Y} \tag{A5}$$

Hence we can write an approximate perturbed solution to problem 13 (see appendix A for details) as:

$$\rho(X,Y) = 1 - \frac{X}{Y} + \epsilon \left(\frac{X^3}{6Y^3} - \frac{X}{6Y}\right) + O(\epsilon^2)$$
(A6)

Now we examine the film thickness:

$$\frac{dY}{d\tau} = -\epsilon \frac{\partial \rho}{\partial X}\Big|_{X=Y(\tau)} \quad ; \quad Y(0) = 0 \tag{A7}$$

Hence, we must solve the separable initial value problem:

$$\frac{dY}{d\tau} = \epsilon \left(\frac{1}{Y}\right) - \epsilon^2 \left(\frac{1}{2Y} - \frac{1}{6Y}\right) \quad ; \quad Y(0) = 0 \tag{A8}$$

The solution is given as:

$$Y(\tau) = \sqrt{2\epsilon\tau - \frac{2}{3}\epsilon^2\tau}$$
 (A9)

Appendix B:

We again seek solutions of the form: $\rho(X,Y) = \rho_0(X,Y) + \epsilon \rho_1(X,Y) + \epsilon^2 \rho_2(X,Y) + \cdots$

The perturbation problem allows us to break this complicated problem into a series of easier problems and we arrive at:

The O(1) problem:

$$0 = \frac{\partial^2 \rho_0}{\partial X^2} - G \frac{\partial \rho_0}{\partial X}$$

$$\rho_0(0, Y) = 1 \quad ; \quad \rho_0(Y, Y) = 0$$
 (B1)

The $O(\epsilon)$ problem:

$$\left(-\frac{\partial \rho_0}{\partial X}\Big|_{X=Y(\tau)}\right) \frac{\partial \rho_0}{\partial Y} = \frac{\partial^2 \rho_1}{\partial X^2} - G \frac{\partial \rho_1}{\partial X}$$

$$\rho_1(0,\tau) = 0 \quad ; \quad \rho_1(Y,Y) = 0$$
(B2)

And so on ...

The solution to the zeroth order problem represented by equation B1 is:

$$\rho_0(X,Y) = 1 + \frac{1 - e^{GX}}{e^{GY} - 1} \tag{B3}$$

Appendix C:

This is a singular perturbation problem and it can be shown that the boundary layer is located at X=Y. Therefore, we first proceed to find the outer solution. The solution for the outer solution comes from setting $\epsilon = 0$ and by satisfying the boundary condition at X=0. Thus we arrive at:

$$\rho_{OUT} = 1 \tag{1C}$$

Within the boundary layer, the approximation is derived by finding the proper scale and renormalizing the coordinate. Hence, we define a stretching variable:

$$\xi = \frac{Y - X}{\epsilon} \tag{2C}$$

Performing a change of variable yields the following problem:

$$\frac{\partial \rho}{\partial Y} \left(\epsilon^2 \frac{\partial \rho}{\partial \xi} \Big|_{\xi=0} \right) = \frac{\partial^2 \rho_{Inner}}{\partial \xi^2} + \frac{\partial \rho_{Inner}}{\partial \xi}$$

$$\rho_{Inner}(\xi=0,\tau) = 0$$
(3C)

This problem has the solution: $\rho_{Inner}(\xi, \tau) = C(1 - e^{-\xi})$

Finally, and to determine C we apply the matching condition:

$$\lim_{\xi \to \infty} \rho_{Inner} = \lim_{X \to 0} \rho_{OUT} \tag{21C}$$

And the uniform solution which is the addition of the inner and outer solutions and subtraction of the common part yields:

$$\rho(x,\tau) = 1 - e^{\left(\frac{X - Y}{\epsilon}\right)} + O(\epsilon)$$
 (22C)

Acknowledgements:

This work was supported as part of the Center for Performance and Design of Nuclear Waste Forms and Containers, an Energy Frontier Research Center funded by the U.S. Department of Energy, Office of Science, Basic Energy Sciences under Award # DE-SC0016584.

References:

- 1. Wagner, C., Z. Phys. Chem., 1933. **25** (B21).
- 2. Cabrera, N. and N.F. Mott, *Theory of the oxidation of metals.* Reports on Progress in Physics, 1949. **12**(1): p. 163.
- 3. Fehlner, F.P. and N.F. Mott, *Low-temperature oxidation*. Oxidation of Metals, 1970. **2**(1): p. 59-99.
- 4. Sato, N. and M. Cohen, *The Kinetics of Anodic Oxidation of Iron in Neutral Solution: I . Steady Growth Region.* Journal of The Electrochemical Society, 1964. **111**(5): p. 512-519.
- 5. Chao, C.Y., L.F. Lin and D.D. Macdonald, *A Point Defect Model for Anodic Passive Films: I . Film Growth Kinetics.* Journal of The Electrochemical Society, 1981. **128**(6): p. 1187-1194.
- 6. Macdonald, D.D., *The history of the Point Defect Model for the passive state: A brief review of film growth aspects.* Electrochimica Acta, 2011. **56**(4): p. 1761-1772.
- 7. Macdonald, D.D., S.R. Biaggio and H. Song, *Steady-State Passive Films: Interfacial Kinetic Effects and Diagnostic Criteria*. Journal of The Electrochemical Society, 1992. **139**(1): p. 170-177.
- 8. Sun, A., J. Franc and D.D. Macdonald, *Growth and Properties of Oxide Films on Platinum: I. EIS and X-Ray Photoelectron Spectroscopy Studies*. Journal of The Electrochemical Society, 2006. **153**(7): p. B260-B277.
- 9. Seyeux, A., V. Maurice and P. Marcus, *Oxide Film Growth Kinetics on Metals and Alloys: I. Physical Model.* Journal of The Electrochemical Society, 2013. **160**(6): p. C189-C196.
- 10. Leistner, K., C. Toulemonde, B. Diawara, et al., *Oxide Film Growth Kinetics on Metals and Alloys: II. Numerical Simulation of Transient Behavior.* Journal of The Electrochemical Society, 2013.

 160(6): p. C197-C205.

- 11. Suo, Y., Z. Zhang and X. Yang, *Perturbation approach to metal surface oxidation considering volume variation*. Advances in Mechanical Engineering, 2017. **9**(1).
- 12. Baroody, H.A., G. Jerkiewicz and M.H. Eikerling, *Modelling oxide formation and growth on platinum*. The Journal of Chemical Physics, 2017. **146**(14): p. 144102.
- 13. Vankeerberghen, M., *1D steady-state finite-element modelling of a bi-carrier one-layer oxide film.* Corrosion Science, 2006. **48**(11): p. 3609-3628.
- 14. Henrich, V.E. and P.A. Cox, *The surface science of metal oxides* 1994, Cambridge: Cambridge University Press.
- 15. Tzvetkoff, T. and J. Kolchakov, *Mechanism of growth, composition and structure of oxide films formed on ferrous alloys in molten salt electrolytes—a review.* Materials Chemistry and Physics, 2004. **87**(1): p. 201-211.
- 16. Chandrasekharan, R., I. Park, R.I. Masel, et al., *Thermal oxidation of tantalum films at various oxidation states from 300 to 700°C.* Journal of Applied Physics, 2005. **98**(11): p. 114908.
- 17. Unutulmazsoy, Y., R. Merkle, D. Fischer, et al., *The oxidation kinetics of thin nickel films between 250 and 500 °C.* Physical Chemistry Chemical Physics, 2017. **19**(13): p. 9045-9052.
- 18. Dighton, A.L. and H.A. Miley, *The Parabolic and Logarithmic Oxidation of Copper*. Transactions of The Electrochemical Society, 1942. **81**(1): p. 321-326.